Laboratory experiments of surf zone dynamics under on-and offshore wind conditions

Damien Sous, Pernille Louise Forsberg, Julien Touboul, Guilherme Gonçalves Nogueira

Laboratory experiments of surf zone dynamics under on- and offshore wind conditions

Damien Sous [a,b], Pernille Louise Forsberg [a], Julien Touboul [a], Guilherme Gonçalves Nogueira[a]

[a] *Université de Toulon, Aix Marseille Université, CNRS, IRD, Mediterranean Institute of Oceanography (MIO), La Garde, France*

[b] *Univ. Pau & Pays Adour, E2S UPPA, SIAME, Anglet, France*

Abstract

This paper presents detailed laboratory experiments investigating the effect onshore and offshore wind conditions have on nearshore wave dynamics, including extreme winds. The experiments were performed using monochromatic waves and a linearly sloping bed. The results show that offshore wind conditions delay wave breaking and promote steep breakers, while onshore wind conditions extend the surf zone and flatten the waves. Firstly, linear and cnoïdal wave models were used in standard formulations to predict the cross-shore wave evolution under no-wind conditions. Secondly, wind effect was added to account for wind-induced modifications of breaker height and energy balance. Despite experimental limitations, the overall satisfactory agreement between theory and observations suggests that such an approach can be used to describe the wind effect in wave nearshore models.

Keywords: Surf zone; wind; Wave breaking height; Wave energy dissipation; Breaker index.

Laboratory experiments of surf zone dynamics under on- and offshore wind conditions

Damien Sous [a,b], Pernille Louise Forsberg [a], Julien Touboul [a], Guilherme Gonçalves Nogueira[a]

[a] *Université de Toulon, Aix Marseille Université, CNRS, IRD, Mediterranean Institute of Oceanography (MIO), La Garde, France*

[b] *Univ. Pau & Pays Adour, E2S UPPA, SIAME, Anglet, France*

1. Introduction

Ocean waves are a dominant driver of nearshore hydrodynamics and beach morphology. A considerable research effort has gone into understanding the linear and non-linear processes that govern wave transformation from deep to shallow water. The most important contributor to nearshore wave dynamics is the shallowing bathymetry, which induces shoaling, refraction, reflection, harmonic transfers, frictional dissipation and breaking of waves (Goda, 1975; Sørensen et al., 1996). Wave breaking is of particular importance because it drives more complex dynamics involving wave setup associated with gradients of radiation stress, circulation, turbulent and frictional dissipation and enhanced non-linear energy transfers to lower frequency "infragravity" waves (Bertin et al., 2018). The complex transformation of the wave field throughout the shoreface will ultimately govern the amount of energy reaching the shore and therefore determine the beach vulnerability to storm and submersion events. Furthermore, waves and wave-induced circulation control the sediment transport and related beach morphodynamics. For example, the non-linearity of waves propagating towards the shore causes the wave shape to change from nearly sinusoidal to skewed and asymmetric (Elgar and Guza, 1985). These processes favour onshore sediment migration under fair weather conditions (Hsu et al., 2006; Grasso et al., 2011).

A variety of approaches and parameterizations have been developed to describe wave transformation in numerical models of nearshore hydro- and morphodynamics (see e.g. Roelvink (1993); Baldock et al. (1998); Janssen and Battjes (2007); Alsina and Baldock (2007); Daly et al. (2012)). A widespread assumption is to use linear wave theory as a basis for the numerical models, which assumes that the wave amplitude remains small relative to the wave length (Airy, 1978). This assumption does not systematically hold true when approaching the breaking point (Martins et al., 2020), in particular for waves with high Irribaren number (Irribarren and Nogales, 1949) i.e. with long waves over steep slopes, or within the surf zone. The cnoïdal-bore model can be a useful alternative to describe the wave shoaling in these cases (see e.g. Svendsen et al. (2003)). Another point of particular interest is the prediction of the breaking point location, which sets the entry point to the surf zone and the related wave energy dissipation. A number of studies have been dedicated to measuring and/or parametrizing the breaker height in relation to offshore wave forcing and bathymetry (see e.g. Komar and Gaughan (1973); Goda (1975, 2010); Rosati et al. (1990); Kamphuis (1991); Smith and Kraus (1991); Shand et al. (2011); Rattanapitikon et al. (2003); Robertson et al. (2013b)). Note that, from a metrological point of view, the identification of the wave breaking point is not a straightforward task (Robertson et al., 2013a; Martins et al., 2017). In the laboratory, experimental measurements of breaker heights can be affected by scaling effects such as applied surface tension, wall friction and surface air-water mixture (Robertson et al., 2013a; Goda and Morinobu, 1998). Furthermore, Laboratory experiments are generally based on regular monochromatic waves, for which breaker height is about 30 % larger than that of irregular waves observed in the field (Goda, 2010). After the breaking point, waves are drastically modified by energy dissipation due to turbulent mixing. A number of models have also been developed to quantify wave energy dissipation in the surf zone (see e.g. Battjes and Janssen (1978); Thornton and Guza (1983); Dally et al. (1985); Roelvink (1993); Baldock et al. (1998); Svendsen et al. (2003); Alsina and Baldock (2007); Janssen and Battjes (2007); Daly et al. (2012)).

Well-known to surfers, sailors and fishermen, strong winds have a straightforward effect on the surf zone. Onshore winds typically favour spilling breakers, which enlarges the surf zone, while offshore winds typically favour plunging breakers, which shortens the surf zone (Galloway et al., 1989). Based on these basic observations, it is to be expected that wind will have a significant effect on the wave breaking height and the subsequent wave energy dissipation, wave-induced circulation and wave impact on the shore. The topic has only received limited attention in the literature, probably due to the technical complexity of combined wind-wave experiments (Liu, 2016). Douglass and Weggel (1989) studied the effect of wind on the shoaling and breaking of waves through a series of experiments in a wave tank equipped with a bidirectional fan at one end. The video-based experiment showed that the wave breaker type, location and index critically depended on the wind speed and direction. The study was helpful to qualitatively understand the effects of wind on the surf zone, but was unable to quantitatively parameterize the surf zone dynamics due to limited data variability. King and Baker (1996) further refined the observations by including wave period and current velocity, which was measured by tracking suspended particles. The study showed that sediment transport was dependent on breaker type, surf zone width and wave breaker height, and concluded that these variables were all influenced by the wind. In more recent experiments, Feddersen and Veron (2005) showed that onshore wind affect the wave dynamics in the shoaling zone, mainly through an increase of the shoaling wave height and an alteration of the wave asymmetry and skewness. Kharif et al. (2008) studied the influence of strong winds on the dynamics of dispersively-focused extreme wave events in deep water, which indicated an increase of momentum and energy transfers and a longer duration of the wave event. Liu (2016) investigated how light wind affects wave breaking and found that even wind-waves generated under low wind speed conditions affect the wave breaking process. Each of these studies highlight the effect of wind on wave transformation in the surf zone, but also calls for a more comprehensive description of the processes under controlled conditions.

The aim of the present study is to quantify the effect of wind on the nearshore wave dynamics. The objectives are to provide a detailed characterisation of wave transformation under on- and offshore wind conditions, including extreme winds, and to analyse the modification of shoaling and breaking processes under controlled conditions. The first part of the paper describes the experimental setup, instrumentation and methods. The second part describes the theoretical model used as a basis formulation to identify and parameterize the effect of wind on wave transformation. The third part presents the results and includes a validation of the theoretical model. The fourth part provides discussion and outlines prospects.

2. Laboratory experiments

2.1. Experimental setup

Wave transformation in the surf zone for onshore, offshore and no-wind conditions were studied in the CASH (Canal Aero-Sedimento-Hydrodynamics) wind-wave flume at the Seatech engineering school, University of Toulon. The flume has a length of 6 m and a width of 0.5 m, and was equipped with a linearly sloping bed (slope 1/20). The still water depth was 0.22 m. Waves were produced as 180 s bursts of regular waves by a piston wave maker in the deep end of the tank. Measurements started after 30s to avoid transitory effects and lasted 120 s at 100 Hz using seventeen resistor type wave gauges set at 0.2 m intervals. The wind tunnel was a closed circuit atmospheric facility producing on- and offshore wind conditions by means of a reversible wind blower (Figure 1). The applied wind speeds ranged from -8 m s^{-1} (offshore) to 8 m s^{-1} (onshore). Four experimental wave cases with different wave characteristics were performed aiming to cover a wide range of wave breaker properties (Table 1). Under no-wind conditions, Wave 1 and Wave 2 were spilling breakers, Wave 3 were transitional between spilling and plunging breakers, while Wave 4 were plunging breakers. For each wind and wave event, four successive runs were performed to ensure robustness in the results.

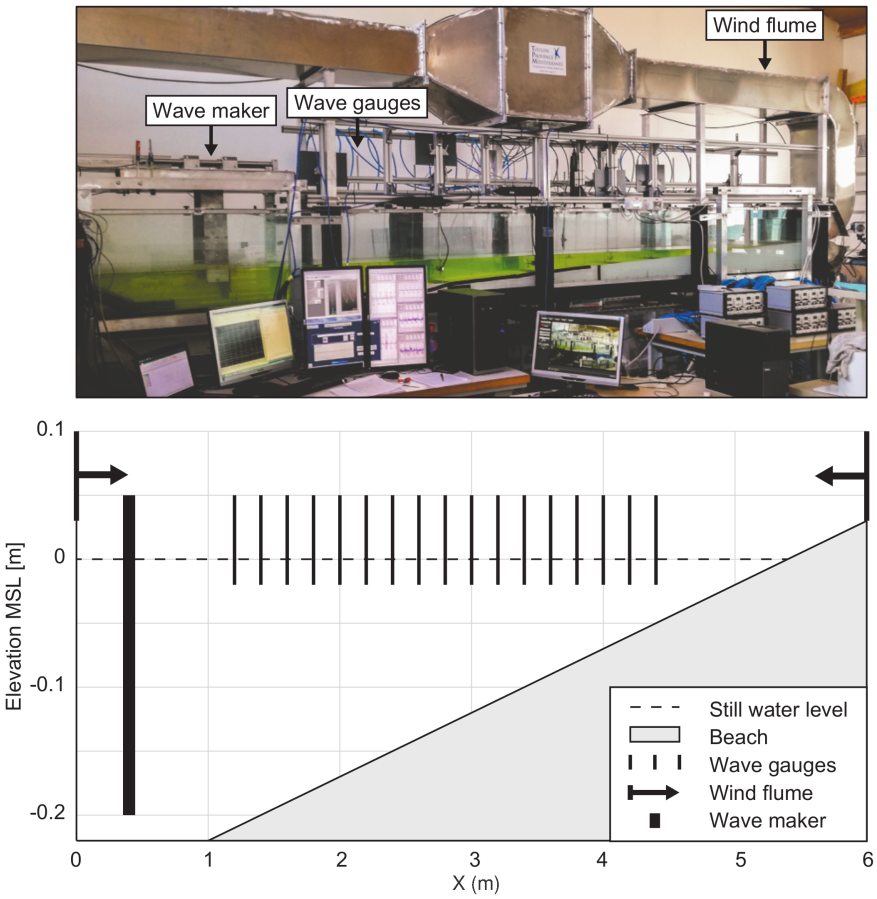

Figure 1: CASH wind-wave flume setup and schematic visualisation.

Table 1: Forcing wave parameters for four regular monochromatic wave cases including wave height closest to the wave maker (H), wave period (T), deep-water wave height (H_o), deep-water wave length (L_o) and surf similarity ($\xi = tan\beta/\sqrt{H/L_o}$) where β is the beach slope.

Scenario	H [m]	T [s]	H_o [m]	L_o [m]	ξ [-]
Wave 1	0.09	0.6	0.093	0.57	0.12
Wave 2	0.07	1.0	0.071	1.56	0.23
Wave 3	0.07	2	0.063	6.23	0.47
Wave 4	0.06	2.4	0.05	8.98	0.61

2.2. Scaling strategy

The laboratory experiments do not aim to provide a comprehensive scaling of natural coastal environments, but rather to characterise the physical processes that govern the wind-wave interaction in nearshore zones under controlled conditions. A range of on- and offshore wind conditions are explored, including extreme winds. The Froude number scaling indicates that the ratio between nature-scaled (W_n) and laboratory (W_l) winds is related to the corresponding geometrical length-scales L_n and L_l:

$$\frac{W_n}{W_l} = \sqrt{\frac{L_n}{L_l}} \tag{1}$$

The geometrical scaling being in the order of 1/20, the laboratory wind speeds of 2, 4, 6 and 8 m s^{-1} correspond to wind speeds of 9, 18, 27 and 36 m s^{-1} or 18, 35, 53 and 70 knots. Note, as for most laboratory

experiments in physical oceanography, a Reynolds number similitude is impossible to achieve.

2.3. Data processing

Data processing was carefully conducted in order to maintain the original wave characteristics while ensuring no wave peak attenuation or phase shift. Outliers were detected and removed through a *Hampel* filter using five neighbouring points and one standard deviation. The data was filtered using a zero-phase low pass filter with a 10 Hz cutoff frequency and 50 dB attenuation.

2.3.1. Forcing wave and statistical parameters

The wave height (H) and period (T) were interpolated from the free surface measurements at the wave gauge closest to the wave maker. From this measurement, the deep-water wave height (H_o) and wave length (L_o) were estimated by linear deshoaling assuming energy flux conservation. The surf similarity parameter (ξ) given in Table 1 was computed based on H, L_o and the slope of the bathymetry. Wave skewness (Equation 2) and wave asymmetry (Equation 3) were estimated based on the water surface fluctuations for each wave gauge with substraction of the mean surface elevation i.e. the zero-mean wave surface elevation (η) and a Hilbert transformation (Hi) through the relations:

$$Sk = \frac{\eta^3}{(\eta^2)^{2/3}} \qquad (2) \qquad\qquad As = \frac{Hi(\eta)^3}{(\eta^2)^{2/3}} \qquad (3)$$

2.3.2. Wave breaking detection

Detecting wave breaking from a cross-shore profile of wave measurements is not a straightforward task. The definition of a universal detection method is still an active research topic (see e.g. Babanin (2011); Itay and Liberzon (2017); Martins et al. (2017); Liberzon et al. (2019)). In the present experiments, the most robust detection method is based on the inflexion of the wave energy profile at the breaking point identified by an increased dissipation after breaking. This is close to the approach used by Bergsma et al. (2019) on bore collapsing. Note that a simple detection of a maximum wave height or energy is not sufficient, since wave dissipation is already observed in the shoaling zone during strong offshore wind conditions. The first step in the present approach is to identify the inflexion point along the mean slope of the squared wave height, which is proportional to the (linear) wave energy. Starting from the shore and moving offshore, linear fits over three points are successively computed until an inflexion is detected. The breaking location and wave height at the breaking point are therefore defined at the intersection of two linear fits over three points located on either sides, as depicted in Figure 2. The difference of the fitted slopes, i.e. the three-points linear cross-shore gradients of the squared wave height for the shoaling and surf zones, were measured. A minimum slope difference of 10 $\mathrm{cm}^2\ \mathrm{m}^{-1}$ was selected as wave breaking criterion. Slope difference values lower than the wave breaking criterion were discarded from the analysis, which for the present experiments represented eight cases out of 144 i.e. 6.25 % of the data. The automatic detection of the wave breaking point was validated with manual measurements carried out during each experiment.

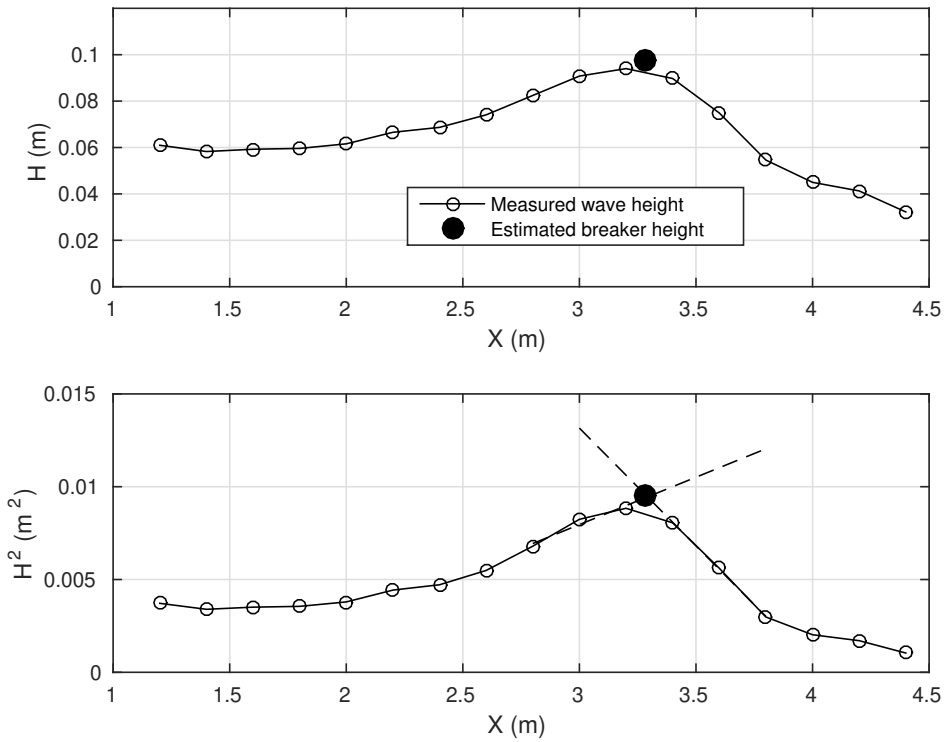

Figure 2: Illustration of the breaking detection procedure. Top: Wave height. Bottom: Squared wave height. Wave breaking (black filled circle) was estimated from the inflexion in the cross-shore profile of squared wave height.

3. Theoretical model

A theoretical model has been developed to describe the wave transformation from the shoaling zone to the end of the surf zone. As is classically done (see e.g. Mei (1989); Baldock et al. (1998); Svendsen et al. (2003); Roelvink et al. (2009)), the model is based on wave averaged energy equation for the oscillatory motion (Phillips, 1966), which reads, for the simple, steady, one-dimensional case considered here,

$$\frac{\partial}{\partial x}\left(\Phi\right) = \mathcal{S} = \mathcal{D} + \mathcal{W}, \tag{4}$$

where Φ refers to an averaged energy flux, and $\mathcal{S}$ is the averaged energy input or dissipation during one wave period. Namely, $\mathcal{S}$ is understood to be the combination effect of the dissipation in the surf zone $\mathcal{D}$, and the energy input due to wind $\mathcal{W}$, which applies in the whole propagation area. The knowledge of these three terms is parametric and various formulations can be found in the literature.

In this work, two formulations were considered to describe the energy flux in the shoaling zone. The difference between these two formulations is based on the domain of validity of the theoretical background underneath. The cases referred to as Wave 1 and Wave 2 in table 1 involve weakly nonlinear water waves initially evolving in intermediate depth and are therefore best described within the framework of linear wave theory. The cases referred to as Wave 3 and Wave 4 involve longer waves leading, on the same bed slope, to higher Iribarren numbers (see Tab. 1), with steeper wave faces before and at breaking. These two cases describe very shallow and high Iribarren water waves, which are better understood within the framework of cnoïdal waves theory. This latter theoretical framework will therefore be considered to describe the averaged energy flux associated with to their propagation.

When considering the surf zone, the breaking process is often considered to be analogous to the situation in a hydraulic jump or a moving bore. Following Svendsen et al. (2003), it makes sense to describe breaking waves through a cnoïdal-bore model.

As was done by Svendsen et al. (1978), a dissipation term $\mathcal{D}$ can also be obtained parametrically. Two different zones have to be considered, i.e. the shoaling zone and the surf zone, where dissipation takes place. Therefore, a breaking criterion has to be considered to segregate these two areas. The formulation considered here is based on Goda's formulation (Goda, 2010).

Finally, the effect of wind is introduced in the two areas considered, and is described within the framework of Jeffreys' theory (Jeffreys, 1925, 1926). These formulations are presented in the following subsections.

3.1. Shoaling zone model

The energy flux Φ described in the previous subsection is analytically defined as

$$\Phi = \overline{\int_{-h_0}^{\xi} \left(p + \frac{1}{2}\rho u^2 \right) dz} \tag{5}$$

Conveniently, and without loss of generality, this expression can be rewritten in a non-dimensional form

$$\Phi = \rho g H^2 c B \tag{6}$$

where H is the wave height, $c = \omega/k$ the phase velocity, and B, the averaged integrand, corresponds to the radiation stress. The explicit computation of c and B requires knowledge of an analytical solution. Thus, a stationary solution was considered, assuming slow variations of the bottom with respect to the wave length.

3.1.1. Linear wave model

Under the assumption of weakly nonlinear water waves, the linear Airy wave theory is often considered (Airy, 1978). From this theory, a very classical analytical solution for water waves propagating in constant depth is known, and can be integrated on depth. Besides, a dispersion equation is associated, which reads:

$$\omega^2 = gk \tanh(kh), \tag{7}$$

This equation can be reformulated in terms of phase velocity:

$$c = \sqrt{\frac{g}{k} \tanh(kh)}. \tag{8}$$

In the meantime, integration of the Bernoulli equation (5) is straightforward, and it comes

$$B = \frac{1}{16} \left(1 + \frac{2kh}{\sinh(2kh)} \right). \tag{9}$$

Knowing c and B, Equation (6) is completely determined. Of course, now that an analytical approximate solution has been considered for integrating B, this formulation can no longer be considered exact.

3.1.2. Cnoïdal wave model

When considering shallow water waves, the cnoïdal wave theory is often an alternative to the linear Airy wave model. The cnoïdal wave theory assumes that the waves are weakly nonlinear Boussinesq waves that are changing so slowly that the local wave shape corresponds to the constant depth solution on that location. In this framework, as is suggested by Svendsen et al. (2003), the solution is determined by the local Ursell number,

$$U_r = \frac{HL^2}{h^3}. \tag{10}$$

Expressing the Ursell number in terms of cnoïdal wave theory leads to the equation

$$U_r = \frac{16}{3} m K(m)^2, \tag{11}$$

where $0 < m < 1$ has to be determined numerically from the equation, and where $K(m)$ is the complete elliptic integral of the first kind. This system has to be solved iteratively, in order to compute the spatial evolution of the Ursell number, and thus the value of the cnoïdal parameter, m. It should be pointed out that full convergence was always obtained for a number of iterations lower than five. The computation of the integrand was performed by (Svendsen, 1974), and we obtained

$$B = \frac{\overline{\eta^2}}{H^2} = \frac{1}{3m^2}\left[\left(1 - 2\frac{E(m)}{K(m)}\right)\left(m - 1 + 2\frac{E(m)}{K(m)}\right) + \left(\frac{E(m)}{K(m)}\right)^2\right], \tag{12}$$

where $E(m)$ is the complete elliptic integral of the second kind.

In the the cnoïdal wave theory framework, the phase speed is found to be

$$\frac{c^2}{gh} = 1 + \left(\frac{2}{m} - 1 - \frac{3E(m)}{mK(m)}\right)\frac{H}{h}. \tag{13}$$

Here again, when c and B are known, equation (6) is fully determined. Since this formulation relies on a different, but still approximate, solution of steady travelling water waves, the solution can no longer be considered exact.

The cnoïdal wave model requires $\frac{L}{c}\sqrt{\frac{g}{h}} > 7$ (Dingemans, 1997). In the present experiment, this range is only reached for Wave 3 and Wave 4 cases. For Wave 1 and Wave 2, $\frac{L}{c}\sqrt{\frac{g}{h}}$ is 4.1 and 6.8, respectively. The cnoïdal model is therefore not applicable, resulting in inconsistent numerical solutions. Only linear wave model will be presented for the Wave 1 and Wave 2 cases.

3.2. Parameterization of wave breaking

A criterion is needed to differentiate the shoaling zone from the surf zone. A breaking criterion is thus introduced. A number of parameterizations are available to predict wave breaking, generally based on Γ_b, the well-known ratio between breaker height H_b and breaking depth h_b, in a wide range of wave and slope conditions (see e.g. Miche (1944); Komar and Gaughan (1973); Weggel (1973); Goda (2010); Liu et al. (2011); Rattanapitikon et al. (2003); Robertson et al. (2013b)). The following analysis is based on Goda's formulation (Goda, 2010) which reads,

$$\Gamma_b = \frac{H_b}{h_b} = \frac{A}{(h_b/L_o)^B}(1 - exp(-1.5\pi\frac{h_b}{L_o}(1 + 11\beta^{4/3}))) \tag{14}$$

where A and B are two empirical constants fixed at 0.17 and 1 by Goda (2010). Slightly different values, namely $A = 0.145$ and $B = 1.05$, are used for the formulation in the present study, based on a best-fit on all no-wind experiments.

3.3. Surf zone model

Strong dissipation is expected to occur in the surf zone. Svendsen et al. (2003) pointed out that the broken waves are very different from classic wave shapes, including linear waves, Stokes waves, stream function waves, or cnoïdal waves. These authors considered that the waves should be considered as propagating bores, or hydraulic jumps. Based on this assumption, a parametric representation of the energy flux Φ and dissipation $\mathcal{D}$ can be provided.

3.3.1. Energy flux in the surf zone

Under the assumption of a bore model, the radiation stress is found to be

$$B = B_0 + \frac{1}{2}\frac{R_a}{H^2}\frac{h}{L}\frac{c^2}{gh} \tag{15}$$

where c refers to a nonlinear phase speed obtained from the bore model, and R_a refers to the roller area. Its value, a constant, is chosen to be $R_a = 0.93$. B_0 has been obtained empirically by Hansen (1990). It is provided by

$$B_0 = B_{0_B}\left\{1 - a\left(b - \frac{h}{h_b}\right)\left(1 - \frac{h}{h_b}\right)\right\}, \tag{16}$$

where

$$a = \frac{1}{15\xi_{00}}$$
$$b = 1.3 - 10\left(\xi_0 - \xi_{00}\right)$$
$$\xi_0 = \frac{h_x}{\sqrt{H_0/L_0}}$$
$$\xi_{00} = \frac{h_x}{\sqrt{0.142}}$$

Svendsen et al. (2003) also obtained an expression of the phase velocity,

$$\frac{c^2}{gh} = 1 + \left(-\frac{3}{2} + 3\frac{\eta_c}{H}\right)\frac{H}{h} + \left(\frac{1}{2} - 3\frac{\eta_c}{H} + 3\frac{\eta_c^2}{H^2}\right)\left(\frac{H}{h}\right)^2 + \left(\frac{1}{2}\frac{\eta_c}{H} - \frac{3}{2}\frac{\eta_c^2}{H^2} + \frac{\eta_c^3}{H^3}\right)\left(\frac{H}{h}\right)^3, \tag{17}$$

Again, the knowledge of c and B provide a full definition of the energy flux Φ.

3.3.2. Energy dissipation in the surf zone

Based on their assumption of a bore model, Svendsen et al. (2003) also provided a parameterization of the dissipated energy:

$$\mathcal{D} = \frac{\rho g H^3}{4hT} D = \frac{\rho g H^3}{4hT} \frac{1}{\left(1 + \frac{\eta_c}{H}\frac{H}{h}\right)\left(1 + \left(\frac{\eta_c}{H} - 1\right)\frac{H}{h}\right)} \tag{18}$$

Hansen (1990) provided the evolution of η_c/H, and suggested that

$$\frac{\eta_c}{H} = 0.5 + \left\{\left(\frac{\eta_c}{H}\right)_B - 0.5\right\}\left(\frac{h}{h_b}\right)^2. \tag{19}$$

where η_c refers to the crest elevation of the breaking wave. Thus, the value of $(\eta_c/H)_B$, the peakedness of the wave at breaking, is found to be an important coefficient. It is computed by assuming that the wave at the breaking point always can be modelled by a cnoïdal wave assumption, which allows the required value to be obtained.

3.4. Wind effect

3.4.1. Wind forcing

The novelty of the present study is to introduce a forcing parameter, describing the action of the wind. The forcing term considered here is based on the Jeffreys' sheltering theory (Jeffreys, 1925, 1926). In his pioneering work, the author introduced a forcing term, describing the asymmetric effect of the pressure on the slope of surface waves. This forcing term was analysed in the context of freak, or rogue waves (Kharif et al., 2008; Touboul et al., 2006; Touboul and Kharif, 2006). In these works, the steep profile of these extreme waves justified the existence of a strong energy input due to the wind. The specific profile of waves in the shoaling zone, and in the surf zone, allow the argument to be extended. Thus, the wind effect is modelled through the relation

$$\mathcal{W} = \frac{1}{8} s \rho_{air} \frac{\omega^2}{c} \|U - c\| (U - c) H^2, \tag{20}$$

where U is the wind speed, and the Jeffreys' sheltering coefficient s, which takes the value $s = 0.25$.

3.4.2. Effect on breaker height

The observations described later on in the present paper reveal a significant influence of the wind on the wave breaking location. The overall effect of wind on Γ_b is taken into account using a wind-related modification of Goda's formulation (Goda, 2010),

$$\Gamma_b^w = (1 - \alpha_w W)\Gamma_b \tag{21}$$

where Γ_b^w is the breaker height to breaking depth ratio in the presence of wind and α_w is an empirical constant fixed at 0.013. More sophisticated parameterizations can be explored in the future, but the aim of the present approach has been to keep the wind effect as simple as possible.

3.5. Comparison between the model and the experiment

Two statistical parameters are used to evaluate the performance of the theoretical model. In the following section, $< . >$ represents the average and $|.|$ represents the modulus.

First, the Root Mean Square Error (RMSE) is the standard deviation of the predicted errors. RMSE is a dimensional error frequently used to evaluate the difference between observed values and predicted values. The lower the RMSE, the better the prediction. RMSE is expressed as,

$$RMSE = \sqrt{< (mod - meas)^2 >} \tag{22}$$

where *mod* and *meas* are the modelled and measured values, respectively. The RMSE is generally not used on its own to assess a model because it is largely influenced by outliers. Willmott (1981) proposed an "index of agreement" defined as

$$WS = 1 - \frac{< (mod - meas)^2 >}{(|mod - < meas >| + |meas - < meas >|)^2} \tag{23}$$

Willmott skill score (WS) of 1 indicates that model and measurements are in perfect agreement. The smaller the WS, the bigger the difference between the numerical model and the observations. This score is dimensionless, and thus complements the information contained in RMSE.

4. Results

4.1. No-wind cases

The theoretical model described above is first tested against measurements of cross-shore wave transformation for no-wind conditions. Figure 3 depicts the compared evolution of wave height across the beach profile for the four studied wave cases. The linear shoaling formulation is used on the four wave cases, while the cnoïdal formulation is only applied on high Irribaren number cases, i.e. Wave 3 and Wave 4 cases.

For Wave 1 and Wave 2, the linear shoaling describes the wave evolution up to the breaking point quite satisfactorily. The shoaling for Wave 1 is associated with a decrease in the wave amplitude, observed in both experimental and theoretical results, which highlights the transition from deep water to intermediate depth conditions. Since this process is very sensitive to the local wave length, the slight theoretical underestimation of the wave decrease is likely due to minor errors in the dispersion relation calculation. The adapted Goda's parameterization (Equation 21) provides a good positioning of the breaking point. To obtain the exact shape of the wave height profile near the breaking point would require a finer approach, but the overall change in the slope is well reproduced. Further onshore, the predicted wave dissipation is also in good agreement with the observations. For Wave 3 and Wave 4, the assumption of linear wave theory in the shoaling zone is clearly no longer valid and the cnoïdal shoaling formulation provides a much better agreement with observations. The breaker location and surf zone dissipation are again well reproduced by the theoretical model.

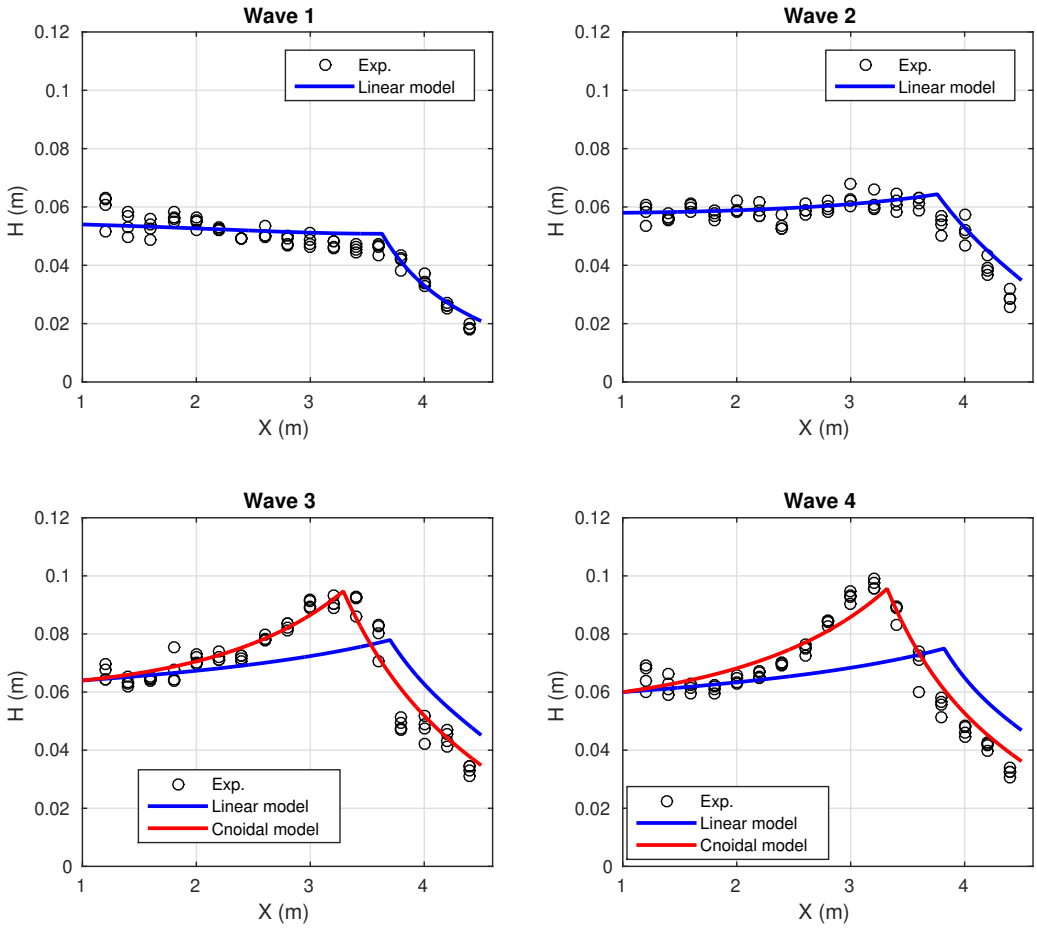

Figure 3: Comparison between theoretical predictions and experimental data for the cross-shore evolution of wave height for the no-wind case. Linear model predictions are depicted for all four wave conditions, while the cnoïdal model results are only given for high Irribaren number cases, i.e. Wave 3 and Wave 4.

Overall, the satisfactory agreement found between predictions and measurements for no-wind cases validates the theoretical approach and its use to characterise the wind influence on wave transformation.

4.2. Wind effect

The experimental data analysis focused on three main issues. First, a typical case was selected to highlight the effect of on- and offshore wind conditions on the cross-shore transformation of wave height, skewness and asymmetry. Second, a focus was placed on the effect of wind on the wave breaking. Finally, complete cross-shore wave transformation under the effect of wind was explored and compared with model predictions.

4.2.1. Overview of wind effect for a selected case

In order to obtain an overview of the wind effect on the cross-shore wave transformation, we focused on a single wave case, Wave 3 (Table 1), during 6 m s^{-1} on- and offshore wind conditions and during no-wind conditions. The first striking observation was the difference in wave height evolution (Figure 4A). During no-wind conditions (green) the wave height showed a slight increase due to shoaling and regular dissipation after breaking, as expected. Onshore wind conditions (blue) tended to increase shoaling, shift the breaking

point offshore and reduce the wave attenuation in the surf zone, while the opposite was observed for offshore wind conditions. Offshore wind conditions (red) postponed wave breaking to shallower depths. Thus, the height-to-depth ratio for wave breaking was highest for offshore wind conditions and lowest for onshore wind conditions.

The cross-shore patterns of wave skewness and asymmetry were also significantly impacted by the wind conditions (Figure 4B,C). During no-wind conditions (green) the wave skewness showed a slow regular increase up to the breaking point followed by a more abrupt decrease within the surf zone. The wave asymmetry initially showed a decreasing trend, probably attributable to an adjustment phase of the wave shape after wave generation, followed by an increasing trend that finally decreased before the breaking point and across the surf zone. These observations in the absence of wind were in good agreement with existing laboratory observations (Grasso et al., 2011). During onshore wind conditions (blue) the wave skewness showed an increase until the breaking point and a decrease after wave breaking with values lower than during no-wind conditions. The wave asymmetry showed a decreasing trend with generally greater asymmetry in both the shoaling and surf zone than during no-wind conditions. These observations quantified the well-know tendency of onshore wind conditions to mash and flatten waves. By contrast, during offshore wind conditions (red), the wave skewness and asymmetry were reduced in the shoaling zone. This could be attributed to a wind drag favouring less skewed waves in the shoaling zone. While this trend cannot be fully explained by the present data, it was confirmed by visual observations during the experiments that the waves slightly flattened and maintained a more sinusoidal shape in the shoaling zone during offshore wind conditions. At the end of the shoaling zone, the depth reduction effect was able to overcome the wind action and induced a rapid increase in both the wave skewness and asymmetry. This resulted in more skewed and asymmetric waves at the breaking point and across the whole surf zone.

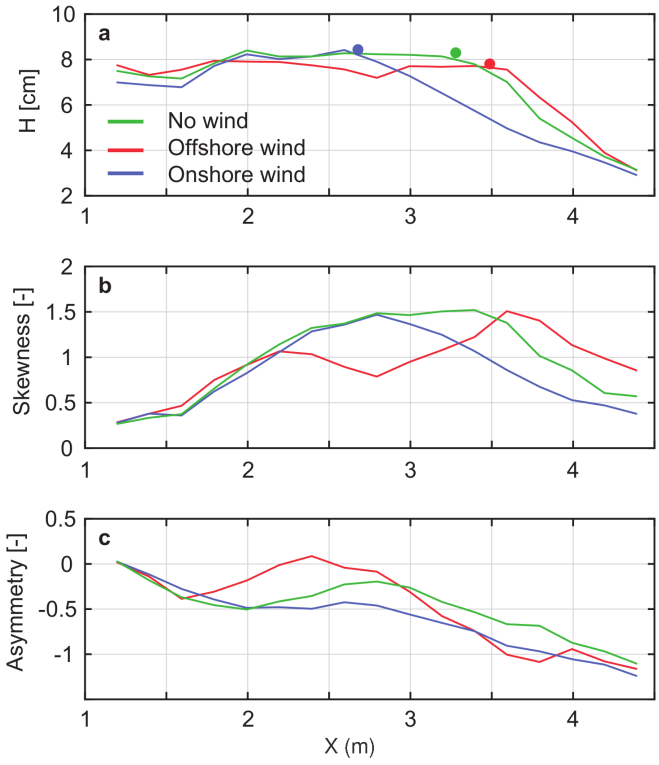

Figure 4: Cross-shore evolution of a) wave height and wave breaking point, b) wave skewness, and c) wave asymmetry for Wave 3 case under no-wind, offshore and onshore wind conditions. A single experimental run is shown for each condition.

4.2.2. Breaking point parameterization

The previous section demonstrated the straightforward effect of wind on the breaking point. The wind effect is taken into account in a modified version of Goda's parameterization (Goda, 2010) of breaker height to breaking depth ratio Γ_b. The formulation is first tested against no-wind conditions. Figure 5A depicts the comparison between measured and predicted Γ_b, namely Γ_{meas} and Γ_{mod}. The original formulation was slightly adapted to provide a better fit for no-wind results, see Section 3.2. Figure 5B shows the ratio $\Gamma_{meas}/\Gamma_{mod}$ for the complete data, including wind conditions. The overall effect of wind is similar to the observations performed previously in this paper, where onshore/offshore winds are associated with earlier/later breaking. The effect of wind on $\Gamma_{meas}/\Gamma_{mod}$ ratio is roughly linear. However a specific behaviour takes place for Wave 2 with an abrupt increase in $\Gamma_{meas}/\Gamma_{mod}$ when the wind is offshore. This observation is probably related to the subtle change in the breaking regime. The overall wind effect on wave breaking led to a significant difference from Goda's parameterization. The wind effect generally increased with wind magnitude and for high Irribaren number waves, see Figure 5B. For the sake of simplicity, the wind effect on breaking is implemented as a linear correction in Goda's formulation (Equation 21). While more complex approaches could provide a finer description of wave breaking in wind conditions, the linear correction applied here is observed to capture most of the wind influence (Figure 5D). The linear correction will therefore be used to trigger wave breaking for all wind conditions in the theoretical results presented in the next section.

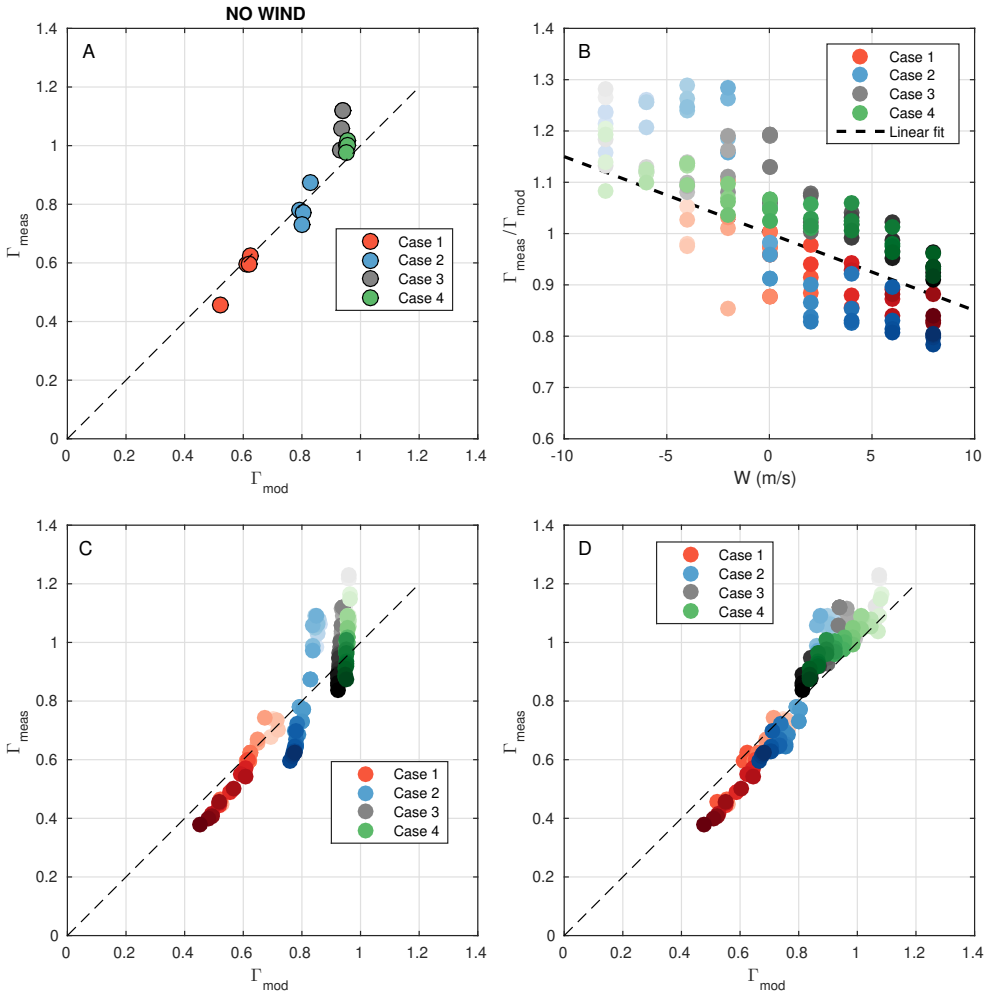

Figure 5: Parameterisation of the breaker height to breaking depth ratio Γ_b. A: comparison between measured Γ_{meas} and predicted Γ_{mod} values for the no-wind cases. B: Ratio $\Gamma_{meas}/\Gamma_{mod}$ vs wind forcing. C: comparison between Γ_{meas} and Γ_{mod} for all cases without implementation of wind effect (colour intensity depicts the wind speed with strong onshore-offshore winds in dark/light colours, see panel B for corresponding wind speed). D: comparison between Γ_{meas} and Γ_{mod} for all cases with implementation of wind effect.

4.2.3. Wave transformation under wind forcing: experiments and theoretical predictions

Figure 6 presents the complete cross-shore wave height profile for a series of selected cases: Wave 2 and Wave 3 in the left and right columns, respectively, and wind speed at -6, -2, 2 and 6 m/s from the top to the bottom rows, respectively. For each case, the results are compared to the same wave case under no-wind conditions including measurements (averaged over four runs performed for each case) and model predictions.

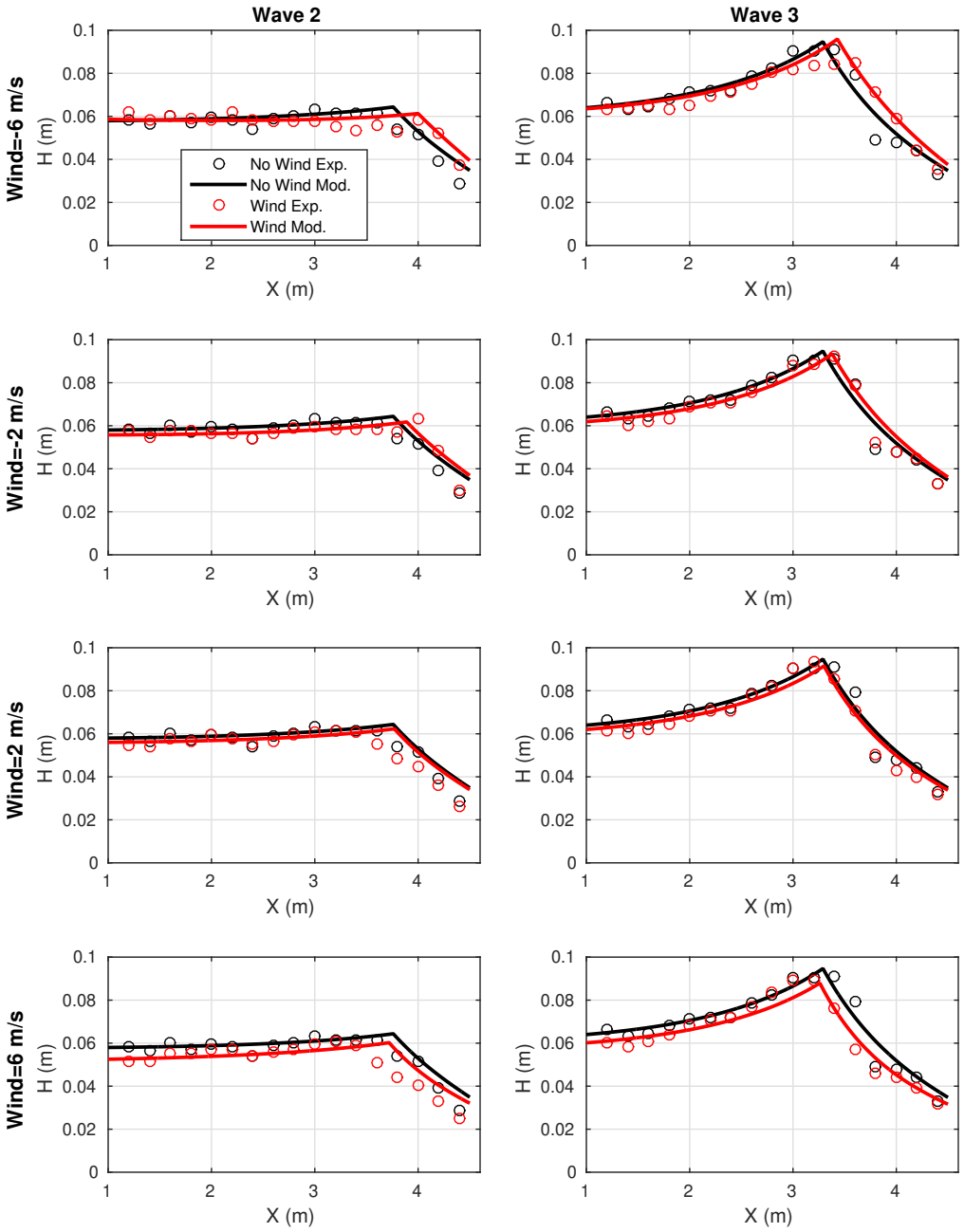

Figure 6: Comparison of theoretical predictions and experimental data for the cross-shore evolution of wave height for Wave 2 and Wave 3. The experimental data is averaged over four runs performed for each wave and wind condition.

The main effects of offshore winds are to postpone the wave breaking and to increase the dissipation in the surf zone. Conversely, onshore winds are observed to shift the breaking point offshore and reduce surf zone dissipation. Offshore winds are also observed to reduce shoaling. This effect can be identified by computing the spatially-averaged wave height between X=2.8 and 3.2 m for Wave 3 case, corresponding to well-shoaled wave area. Offshore winds of -2 and -6 m/s lead to a decrease of the spatially-averaged wave height of 0.21

and 0.58 cm, respectively. For onshore wind, the wind-effect on the shoaling zone is not measurable. Overall, the wind effects on the wave field are well captured by the model. The main difference between the model and the measurements are observed during in strong offshore wind conditions, where the model tends to overestimate the wave height just before breaking, and during onshore winds conditions for Wave 2, where modelled breaking occurs later than measured. In both cases, small scale processes related to wave crest instability, which are not explicitly represented by the theoretical model, are expected to locally affect the nearshore breaking wave dynamics.

Statistical error parameters are used to quantify the difference between model prediction and measurements. Figure 7 depicts the Root Mean Squared Error (RMSE) and the Willmott Score (WS) against wind speed for the four wave cases (top to bottom Wave 1 to Wave 4). For each plot the experimental data is the averaged data over four runs performed in each wave and wind condition. The model prediction given by the no-wind theoretical approach is clearly impaired when wind is present. The error generally grows with increasing wind magnitude. The error statistics confirm the previous observations of a clear improvement in the theoretical predictions when including the wind effect in both the wave breaking point and the wind-wave energy transfers. The sensitivity to wind effect observed is higher for low Irribaren wave cases, i.e. Wave 1 and 2, than for transitional to plunging wave conditions, i.e. Wave 3 and 4.

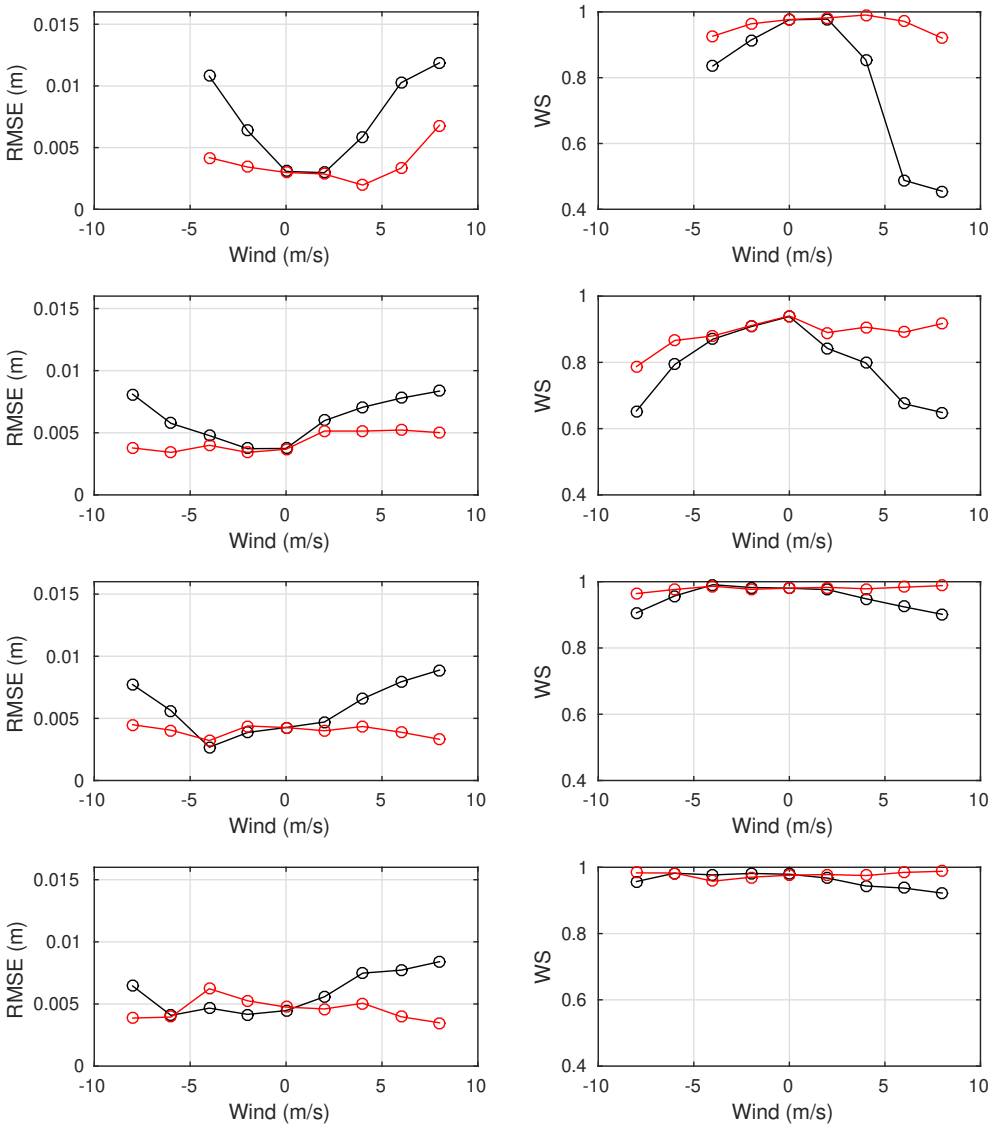

Figure 7: Root Mean Squared Errors (RMSE) and Willmott Score (WS) for the four wave cases vs wind forcing, from top to bottom Wave 1 to Wave 4.

5. Discussion

Building on previous research on wind-wave interactions (Galloway et al., 1989; Douglass and Weggel, 1989; King and Baker, 1996; Feddersen and Veron, 2005), this study presents a detailed quantification of the wind effect on surf zone dynamics in a controlled environment for both on- and offshore wind conditions, including very strong wind conditions. The experimental results confirm the existing empirical *in-situ* knowledge and previous laboratory observations (Douglass and Weggel, 1989; King and Baker, 1996) that offshore wind conditions tend to postpone the breaking point and promote steep breakers, while onshore wind

conditions tend to spread out the surf zone and flatten waves. Significant modifications of the wave shape are observed. In the shoaling zone, the transfer of wind energy to the wave field is observed to increase/decrease the wave height for onshore/offshore wind conditions, confirming the onshore wind observations of Feddersen and Veron (2005). A theoretical model, based on linear or cnoïdal wave theory and Goda's parameterization (Goda, 2010) for wave breaking, showed good accuracy in reproducing wave transformation under no-wind conditions. However, the wind-induced wave field modifications significantly impaired the model performance. Two improvements have been proposed to account for the wind effect: (i) the wind-wave energy transfer according to Jeffrey's theory, and (ii) a modified expression of the breaking point parameterization. While a number of small-scale processes, such as the development of micro-breakers (Douglass and Weggel, 1989) are ignored by this bulk approach of wind effect, these two modifications bring a significant improvement to the model accuracy for both on- and offshore wave conditions. In line with the analysis of Feddersen and Veron (2005), this confirms that the wind effect on wave shape is governed by wind-wave interactions along the wave propagation rather than by the exclusive wave height modification effect.

The present observations call for a series of remarks and open up new prospects. First, the dynamics of wind-wave interaction near the breaking point must be refined. By contrast with the observations of King and Baker (1996) under moderate wind conditions, the present experiments demonstrate that, for strong wind conditions, the breaker height to depth ratio is not only affected by the changes in breaker depth but also by the wave height at breaking. The simple wind-modified parameterization of breaker height proposed here should be a good starting point to include the wind effect in nearshore wave models, but further efforts are required to provide a more accurate description of the on- and offshore wind effect on wave breaking. It should be noted that, in the laboratory framework, the wave breaking point detection remains a delicate issue and affects the subsequent parameterization process. Small scale processes involved in the wave crest dynamics near the breaking point cannot be fully explained by the present study. It would probably require advanced high resolution numerical simulations of the individual waves (see e.g. Xie (2017)). The wind effect on wave breaking, with the global trend to promote earlier spilling-type breaking and later plunging-type breaking for onshore/offshore winds, respectively, is attributed to the surface shear induced by the wind. Onshore/offshore winds will generate opposite vorticity in the surface layer, therefore forcing/preventing the onset of breaking (King and Baker, 1996; Longuet-Higgins, 1994). The range of wind speeds applied in the present experiments demonstrate that even plunging waves can be affected by wind, in contrast to the observations of King and Baker (1996) under moderate wind conditions. The dynamics of wave breaking in the presence of wind should be envisioned as a coupled air-water processes. The modification of the shoaling and breaking wave shape will in turn modify the air flow pattern around the crest and consequently affect the related pressure drag and surface shear applied to the wave. Air flows around wave crests have been documented early on (Wu, 1968, 1969), showing in particular that air flow separation is generally associated with the occurrence of wave breaking (Banner and Melville, 1976; Kawai, 1981; Kharif et al., 2008; Tian and Choi, 2013). However, most of these results have been obtained for deep-water waves under moderate onshore wind forcing conditions. Wave-air flow interactions remains to be fully explored under strong winds, offshore winds, shallow water waves and bathymetry-induced wave breaking. The present experimental results should provide useful benchmark cases to test future theoretical and numerical works.

A second major issue is the extrapolation of the present observations and theoretical approach to a more realistic context. The beach slope (1:20) is quite steep, i.e. generally corresponding to reflective gravel beaches in the field. The assumption of a slowly varying wave field in the shoaling zone is not valid. However, as argued by Feddersen and Veron (2005), the wind effect over smaller beach slope is expected to increase due to a larger propagation distance over which to interact. Applying Froude scaling to the present experiments, our observations should correspond to wind speeds between 9 and 36 m/s, i.e. from moderate breeze to violent storm regimes. The wind effect on the wave dynamics has been observed for each case, including the low wind cases. This indicates that modifications in the wave field across shoaling and surf zones is expected in the field even for moderate breeze conditions. Inertial and turbulent effects cannot be scaled at the small-scale laboratory (Thornton et al., 2000). Considering the technical and operating costs of near-prototype scale experiments on nearshore wave dynamics (see e.g. Williams et al. (2012); Yoon and Cox (2010)), the inclusion of a bi-directional wind flume to the existing beach-scale installations to explore wind effect at the real beach scale may remain out of reach for the next few years. In addition, the present experiments were

performed with the simplest approach in order to single out the effect of wind on the surf zone dynamics, i.e. with a flat linear beach and monochromatic waves. Further tests at laboratory scale are required with more realistic beach profiles and wave spectra to confirm the robustness of the present observations. The next step will then be to compare the model with field observations, with all implied difficulties in terms of experimental control. However, keeping in mind the limitations, it seems reasonable that the observed physical processes should remain valid under more complex conditions, and that the present approach may remain useful for the implementation of wind effects in nearshore models. In particular, the striking wind effect on breaker height and location should not be ignored in nearshore areas exposed to strong winds.

The effects of on- and offshore wind conditions on the surf zone dynamics, i.e. shifted wave breaking point, modified wave energy dissipation and modified wave skewness and asymmetry may imply strong consequences for sediment transport (Hsu et al., 2006; Marino-Tapia et al., 2007; Grasso et al., 2011). Many beaches around the world are exposed to strong wind conditions, being regular (e.g. trade winds) or changing either periodically (diurnal sea breeze cycles) or intermittently under the fluctuations in synoptic wind conditions. Therefore wind action over the shoaling and surf zones should be an important driving mechanism for beach equilibrium profiles. Ignoring the wind effect in nearshore hydro-morphodynamical models, in particular the change in wave shape, would result in incorrect beach morphodynamics predictions (Feddersen and Veron, 2005).

6. Conclusion

Strong winds are well-known to affect the ocean wave dynamics. This is particularly visible nearshore, where wave breaking characteristics can drastically differ between onshore and offshore wind conditions. The present study aimed at providing a quantification of the wind effect on the wave dynamics in the shoaling and surf zones using controlled laboratory experiments under on- and offshore wind conditions including very strong winds. Onshore winds were observed to extend the surf zone by shifting the breaking point seaward and to flatten waves. By contrast, offshore winds were observed to postpone the breaking point toward the shore, thus producing steeper wave faces. Similar trends are observed for linear and non-linear waves, with the surf-similarity parameter ranging from 0.12 to 0.61. These results are a clear quantitative confirmation under controlled laboratory conditions of classical visual observations of real-world surf zone. A wave propagation model, based on classical linear and cnoïdal wave theories, has been built to assess how laboratory wave transformation can be predicted by usual theoretical approaches. The wind-induced modifications of shoaling and breaking wave dynamics were taken into account in a theoretical approach by including a wind input term in the wave averaged energy equation based on the Jeffrey's sheltering theory (Jeffreys, 1925) and by adding a wind effect in the parameterization of breaker height. The wave model shows satisfactory predictive capacity, with the wind effect being overall well represented. Additional research should be undetaken to further explore the validity of the proposed approach, including irregular wave forcing, more complex bathymetry and comparison with field measurements, before this approach can be implemented in nearshore wave models.

Acknowledgements

The authors would like to thank Aimed Ajroud for his participation in the laboratory experiments. The Gladys group supported the experiments.

References

Airy, G., 1978. Tides and waves. In: Encyclopædia Metropolitana. Vol. 3. Cambridge Philosophical Society.

Alsina, J., Baldock, T., 2007. Improved representation of breaking wave energy dissipation in parametric wave transformation models. Coastal Engineering 54 (10), 765–769.

Babanin, A., 2011. Breaking and dissipation of ocean surface waves. Cambridge University Press.

Baldock, T., Holmes, P., Bunker, S., Van Weert, P., 1998. Cross-shore hydrodynamics within an unsaturated surf zone. Coastal Engineering 34 (3-4), 173–196.

Banner, M. L., Melville, W. K., 1976. On the separation of air flow over water waves. Journal of fluid mechanics 77 (4), 825–842.

Battjes, J. A., Janssen, J., 1978. Energy loss and set-up due to breaking of random waves. In: Coastal Engineering. pp. 569–587.

Bergsma, E. W., Blenkinsopp, C. E., Martins, K., Almar, R., de Almeida, L. P. M., 2019. Bore collapse and wave run-up on a sandy beach. Continental Shelf Research 174, 132–139.

Bertin, X., De Bakker, A., Van Dongeren, A., Coco, G., Andre, G., Ardhuin, F., Bonneton, P., Bouchette, F., Castelle, B., Crawford, W. C., et al., 2018. Infragravity waves: From driving mechanisms to impacts. Earth-Science Reviews.

Dally, W. R., Dean, R. G., Dalrymple, R. A., 1985. Wave height variation across beaches of arbitrary profile. Journal of Geophysical Research: Oceans 90 (C6), 11917–11927.

Daly, C., Roelvink, D., van Dongeren, A., de Vries, J. v. T., McCall, R., 2012. Validation of an advective-deterministic approach to short wave breaking in a surf-beat model. Coastal Engineering 60, 69–83.

Dingemans, M. W., 1997. Water wave propagation over uneven bottoms. Vol. 13. World Scientific.

Douglass, S. L., Weggel, J. R., 1989. Laboratory experiments on the influence of wind on nearshore wave breaking. In: Coastal Engineering. pp. 632–643.

Elgar, S., Guza, R., 1985. Observations of bispectra of shoaling surface gravity waves. Journal of Fluid Mechanics 161, 425–448.

Feddersen, F., Veron, F., 2005. Wind effects on shoaling wave shape. Journal of physical oceanography 35 (7), 1223–1228.

Galloway, J., Collins, M., Moran, A., 1989. Onshore/offshore wind influence on breaking waves: an empirical study. Coastal Engineering 13 (4), 305–323.

Goda, Y., 1975. Irregular wave deformation in the surf zone. Coastal Engineering in Japan 18 (1), 13–26.

Goda, Y., 2010. Reanalysis of regular and random breaking wave statistics. Coastal Engineering Journal 52 (01), 71–106.

Goda, Y., Morinobu, K., 1998. Breaking wave heights on horizontal bed affected by approach slope. Coastal Engineering Journal 40 (04), 307–326.

Grasso, F., Michallet, H., Barthélemy, E., 2011. Sediment transport associated with morphological beach changes forced by irregular asymmetric, skewed waves. Journal of Geophysical Research: Oceans 116 (C3).

Hansen, J. B., 1990. Periodic waves in the surfzone: analysis of experimental data. Coast. Eng. 14, 19–41.

Hsu, T.-J., Elgar, S., Guza, R., 2006. Wave-induced sediment transport and onshore sandbar migration. Coastal Engineering 53 (10), 817–824.

Irribarren, C., Nogales, C., 1949. Protection des ports. In: XVII, International Navigation Congress, Section II, Comm. Vol. 4. pp. 27–47.

Itay, U., Liberzon, D., 2017. Lagrangian kinematic criterion for the breaking of shoaling waves. Journal of Physical Oceanography 47 (4), 827–833.

Janssen, T., Battjes, J., 2007. A note on wave energy dissipation over steep beaches. Coastal Engineering 54 (9), 711–716.

Jeffreys, H., 1925. On the formation of wave by wind. Proc. Roy. Soc. A 107, 189–206.

Jeffreys, H., 1926. On the formation of wave by wind (second paper). Proc. Roy. Soc. A 110, 241–247.

Kamphuis, J., 1991. Incipient wave breaking. Coastal Engineering 15 (3), 185–203.

Kawai, S., 1981. Visualization of airflow separation over wind-wave crests under moderate wind. Boundary-Layer Meteorology 21 (1), 93–104.

Kharif, C., Giovanangeli, J.-P., Touboul, J., Grare, L., Pelinovsky, E., 2008. Influence of wind on extreme wave events: experimental and numerical approaches. Journal of Fluid Mechanics 594, 209–247.

King, D., Baker, C., 1996. Changes to wave parameters in the surf zone due to wind effects. Journal of Hydraulic Research 34 (1), 55–76.

Komar, P. D., Gaughan, M. K., 1973. Airy wave theory and breaker height prediction. In: Coastal Engineering 1972. pp. 405–418.

Liberzon, D., Vreme, A., Knobler, S., Bentwich, I., 2019. Detection of breaking waves in single wave gauge records of surface elevation fluctuations. Journal of Atmospheric and Oceanic Technology 36 (9), 1863–1879.

Liu, X., 2016. A laboratory study of spilling breakers in the presence of light-wind and surfactants. Journal of Geophysical Research: Oceans 121 (3), 1846–1865.

Liu, Y., Niu, X., Yu, X., 2011. A new predictive formula for inception of regular wave breaking. Coastal Engineering 58 (9), 877–889.

Longuet-Higgins, M. S., 1994. Shear instability in spilling breakers. Proceedings of the Royal Society of London. Series A: Mathematical and Physical Sciences 446 (1927), 399–409.

Marino-Tapia, I., Russell, P., O'Hare, T., Davidson, M., Huntley, D., 2007. Cross-shore sediment transport on natural beaches and its relation to sandbar migration patterns: 1. field observations and derivation of a transport parameterization. Journal of Geophysical Research: Oceans 112 (C3).

Martins, K., Blenkinsopp, C. E., Power, H. E., Bruder, B., Puleo, J. A., Bergsma, E. W., 2017. High-resolution monitoring of wave transformation in the surf zone using a lidar scanner array. Coastal Engineering 128, 37–43.

Martins, K., Bonneton, P., Mouragues, A., Castelle, B., 2020. Non-hydrostatic, non-linear processes in the surf zone. Journal of Geophysical Research: Oceans, e2019JC015521.

Mei, C. C., 1989. The applied dynamics of ocean surface waves. Vol. 1. World scientific.

Miche, M., 1944. Mouvements ondulatoires de la mer en profondeur constante ou décroissante. Annales de Ponts et Chaussées, 1944, pp (1) 26-78,(2) 270-292,(3) 369-406.

Phillips, O. M., 1966. The Dynamics of the Upper Ocean. Cambridge Univ. Press.

Rattanapitikon, W., Vivattanasirisak, T., Shibayama, T., 2003. A proposal of new breaker height formula. Coastal engineering journal 45 (1), 29–48.

Robertson, B., Hall, K., Nistor, I., Zytner, R., Storlazzi, C., 2013a. Remote sensing of irregular breaking wave parameters in field conditions. Journal of Coastal Research 31 (2), 348–363.

Robertson, B., Hall, K., Zytner, R., Nistor, I., 2013b. Breaking waves: Review of characteristic relationships. Coastal Engineering Journal 55 (01), 1350002.

Roelvink, D., Reniers, A., Van Dongeren, A., de Vries, J. v. T., McCall, R., Lescinski, J., 2009. Modelling storm impacts on beaches, dunes and barrier islands. Coastal engineering 56 (11-12), 1133–1152.

Roelvink, J., 1993. Dissipation in random wave groups incident on a beach. Coastal Engineering 19 (1-2), 127–150.

Rosati, J. D., Gingerich, K. J., Kraus, N. C., 1990. Superduck surf zone sand transport experiment. Tech. rep., Coastal Engineering Research Center Vicksburg MS.

Shand, T. D., Bailey, D. G., Shand, R. D., 2011. Automated detection of breaking wave height using an optical technique. Journal of Coastal Research 28 (3), 671–682.

Smith, E. R., Kraus, N. C., 1991. Laboratory study of wave-breaking over bars and artificial reefs. Journal of waterway, port, coastal, and ocean engineering 117 (4), 307–325.

Svendsen, I. A., 1974. Cnoidal waves over a gently sloping bottom. In: Inst. Hydrodyn. Hydraul. Eng. (ISVA). Tech. Univ. Denmark, Lyngby.

Svendsen, I. A., Madsen, P. A., Hansen, J. B., 1978. Wave characteristics in the surf zone. In: ASCE Proc. 16th Int. Conf. Coastal Engineering. Hamburg, pp. 520–539.

Svendsen, I. A., Qin, W., Ebersole, B. A., 2003. Modelling waves and currents at the lstf and other laboratory facilities. Coastal Engineering 50 (1-2), 19–45.

Sørensen, O., Madsen, P., Schäffer, H., 1996. Nonlinear wave dynamics in the surf zone. In: Coastal Engineering. pp. 1178–1191.

Thornton, E., Dalrymple, T., Drake, T., Elgar, S., Gallagher, E., Guza, R., Hay, A., Holman, R., Kaihatu, J., Lippmann, T., et al., 2000. State of nearshore processes research: Ii. report based on the nearshore research workshop, st. petersburg, florida. Tech. rep., September 14-16, 1998. Technical report NPS-OC-00-001. Naval Postgraduate ....

Thornton, E. B., Guza, R., 1983. Transformation of wave height distribution. Journal of Geophysical Research: Oceans 88 (C10), 5925–5938.

Tian, Z., Choi, W., 2013. Evolution of deep-water waves under wind forcing and wave breaking effects: Numerical simulations and experimental assessment. European Journal of Mechanics-B/Fluids 41, 11–22.

Touboul, J., Giovanangeli, J. P., Kharif, C., Pelinovski, E., 2006. Freak waves under the action of wind : Experiments and simulations. Eur. J. Mech., B. Fluids 25, 662–676.

Touboul, J., Kharif, C., 2006. On the interaction of wind and extreme gravity waves due to modulational instability. Phys. Fluids 18, 108103.

Weggel, J. R., 1973. Maximum breaker height for design. In: Coastal Engineering 1972. pp. 419–432.

Williams, J., Buscombe, D., Masselink, G., Turner, I., Swinkels, C., 2012. Barrier dynamics experiment (bardex): Aims, design and procedures. Coastal Engineering 63, 3–12.

Willmott, C. J., 1981. On the validation of models. Physical geography 2 (2), 184–194.

Wu, J., 1968. Laboratory studies of wind–wave interactions. Journal of Fluid Mechanics 34 (1), 91–111.

Wu, J., 1969. A criterion for determining air-flow separation from wind waves. Tellus 21 (5), 707–714.

Xie, Z., 2017. Numerical modelling of wind effects on breaking waves in the surf zone. Ocean Dynamics 67 (10), 1251–1261.

Yoon, H.-D., Cox, D. T., 2010. Large-scale laboratory observations of wave breaking turbulence over an evolving beach. Journal of Geophysical Research: Oceans 115 (C10).